Direct numerical simulation study of a turbulent stably stratified air flow above the wavy water surface.

O.A. Druzhinin[1,2] and Yu.I. Troitskaya[1,2]

[1] The Institute of Applied Physics, Russian Acad. Sci., Nizhny Novgorod, Russia
[2] University of Nizhny Novgorod, Nizhny Novgorod, Russia
druzhinin@hydro.appl.sci-nnov.ru

Introduction. Investigation of the interaction of surface water waves with the wind flow is of primary importance for the parameterization of turbulent momentum and heat fluxes in the turbulent boundary layer (BL) over the water surface [1]. The most difficult case for modeling is that of steep waves, when the strongly non-linear effects (e.g. sheltering, flow separation, vortex formation etc.) are encountered in the airflow over waves [2]. Of special interest is also the influence of the wind flow stratification on the properties of the BL flow [3]. In the present work the detailed structure and statistical characteristics of a turbulent, stably stratified atmospheric boundary layer over waved water surface are studied by direct numerical simulation (DNS) [4]. In DNS two-dimensional water waves with different wave age parameters (c/u_* = 0-10, where u_* is the friction velocity and c is the wave celerity), wave slope up to ka = 0.2 and at a bulk Reynolds number from Re = 15000 for ka = 0.2 to Re = 80000 for a flat surface, and different values of the bulk Richardson number Ri (based on the buoyancy jump, bulk velocity and the surface wave length) are considered. The shape of the water wave is prescribed and does not evolve under the action of the wind. The full, 3D Navier-Stokes equations under the Boussinesq approximation are solved in curvilinear coordinates in a frame of reference moving the phase velocity of the wave. The shear driving the flow is created by an upper plane boundary moving horizontally with a bulk velocity in the x-direction. Periodic boundary conditions are considered in the horizontal (x) and lateral (y) directions, and no-slip boundary condition is considered in the vertical z-direction. Ensemble-averaged velocity and pressure fields are evaluated by averaging over time and the spanwise coordinate. Profiles of the mean velocity and turbulent stresses are obtained by averaging over wavelength.

The DNS results show that the wind flow is significantly affected by stratification. If the Richardson number is sufficiently small, there exists a statistically stationary, turbulent BL flow regime. On the other hand, if the Richardson number is sufficiently large the wind flow turbulence is suppressed under the stabilizing effect of stratification, and velocity fluctuations in the BL decay to zero, in the case of a sufficiently small wave slope. However, the velocity fluctuations remain finite (non-zero) the wave slope is sufficiently large. Hence, the BL turbulence is "pumped" by the surface wave in this case.

Basic equations and numerical method. We perform direct numerical simulation of a turbulent stably stratified BL flow above the wavy water surface. The schematic of the numerical experiment is presented in Fig. 1. A Cartesian framework is considered where x-axis is oriented along the mean wind flow, z-axis is directed vertically upwards and y-axis is transversal to the mean flow and parallel to the wave front. A two-dimensional water wave is considered with amplitude a, wavelength λ and phase velocity c, and periodical in the x-direction. In the present study a maximum wave slope is $ka = 2\pi a/\lambda$ = 0.2. DNS is performed in a reference frame moving with the wave phase velocity, so that the horizontal coordinate in the moving framework is $x = x' - ct$, where x' is the coordinate in the laboratory reference frame. Therefore, in the moving reference frame, the lower boundary representing the wave surface is stationary. A no-slip boundary condition is considered at the lower boundary, so that the wind flow velocity at this boundary coincides with the orbital velocities of particles in the water wave and is independent of time. The computational domain with sizes $L_x = 6\lambda$, $L_y = 4\lambda$ and $L_z = \lambda$ in the x-, y-, and z-directions is considered, and the wind flow is assumed to be periodical in the x- and y-directions. Also a no-slip boundary condition is prescribed at the upper horizontal plane which is assumed to be moving with bulk velocity U_0 in the x-direction. This condition provides external momentum source due to the action of the viscous shear stress which compensates the viscous dissipation in BL and makes the

flow statistically stationary. Thus, for a flat lower boundary the flow is identical to a turbulent Couette flow. In order to establish a stable density stratification of the flow we prescribe the

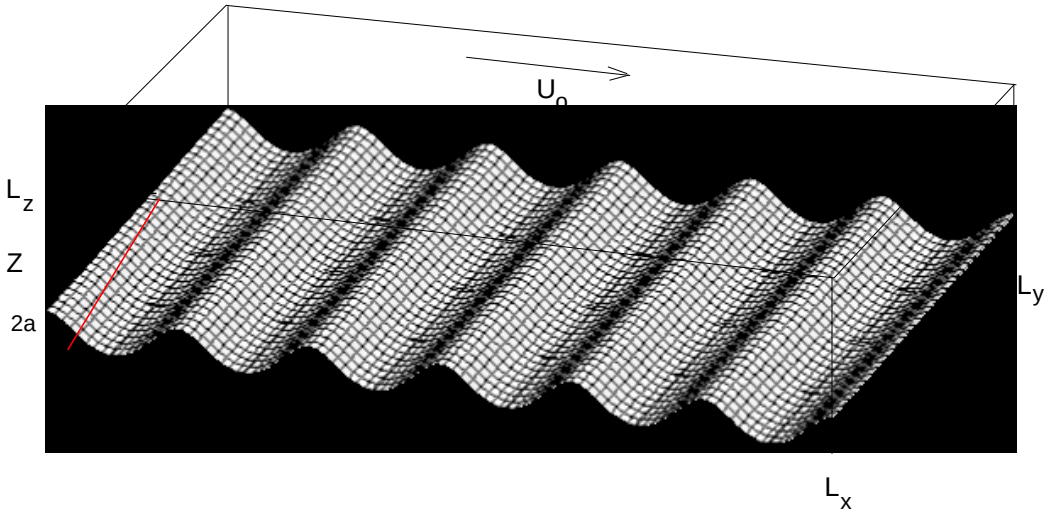

Fig. 1.

temperature at the top and bottom boundary planes, T_1 at $z = 0$ and T_2 at $z = L_z$ where $T_1 < T_2$.

Numerical algorithm is based on the integration of full, 3D Navier-Stokes equations for an incompressible fluid. In the dimensionless variables, the governing equations are written in the form [5]:

$$\frac{\partial U_i}{\partial t} + \frac{\partial (U_i U_j)}{\partial x_j} = -\frac{\partial P}{\partial x_j} + \frac{1}{\mathrm{Re}} \frac{\partial^2 U_i}{\partial x_j \partial x_j} + \delta_{iz} Ri \widetilde{T} f(t) \tag{1}$$

$$\frac{\partial U_j}{\partial x_j} = 0. \tag{2}$$

$$\frac{\partial \widetilde{T}}{\partial t} + \frac{\partial (U_j \widetilde{T})}{\partial x_j} + U_z = \frac{1}{\mathrm{PrRe}} \frac{\partial^2 \widetilde{T}}{\partial x_j \partial x_j} \tag{3}$$

where $U_i (i = x, y, z)$ are the velocity components, P is the pressure and $\widetilde{T}$ the deviation of the temperature from a linear reference profile $(1 + z)$. Thus, the full dimensionless temperature is given by $T = 1 + z + \widetilde{T}$. The variables in (1)-(3) are normalized by the wavelength λ and velocity U_0 and the temperature difference $T_2 - T_1$, and the pressure is normalized by ρU_0^2 (where ρ is the air density). The bulk Reynolds and Richardson numbers are defined as

$$\mathrm{Re} = \frac{U_0 \lambda}{\nu} \tag{4}$$

$$\mathrm{Ri} = g \frac{T_2 - T_1}{T_1} \frac{\lambda}{U_0^2} \tag{5}$$

where ν is the kinematic air viscosity and g the gravity acceleration. The Prandl number, $\mathrm{Pr} = \nu / \kappa$ (where κ is thermal diffusivity), is prescribed as $\mathrm{Pr} = 0.7$. Factor f in the last term in the r.h.s. of (1) is introduced in the form

$$f(t) = 1 - \exp(-t/100) \tag{6}$$

where t is the dimensionless time variable. This function "switches" on the stabilizing effect of stratification is such a way that the turbulent, non-stratified Couette flow regime is allowed to develop at times $t < 100$.

In order to avoid the strong geometrical non-linearity during integration of (1) - (3) related to the bottom wavy boundary (Fig. 1), a conformal mapping is employed which transforms the plane (x,z) in the Cartesian frame to a plane (ξ, η) in curvilinear coordinates as:

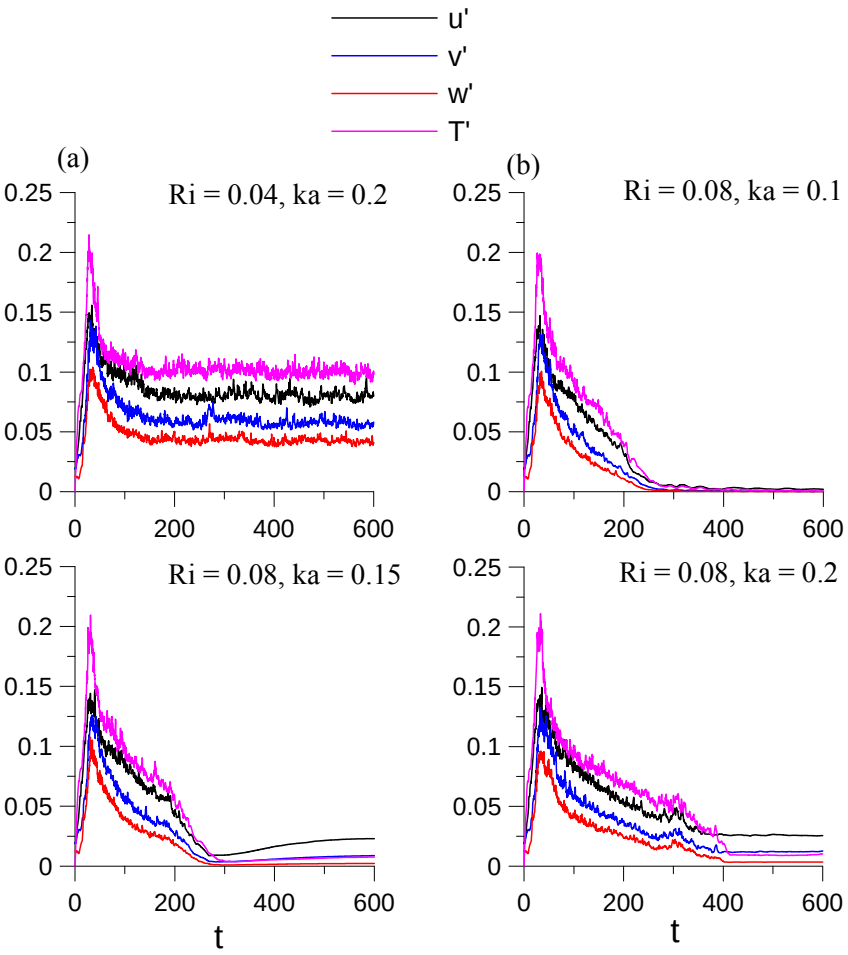

Fig. 2.

$$x = \xi - a\exp(-k\eta)\sin k\xi \tag{7}$$

$$z = \eta + a\exp(-k\eta)\cos k\xi \tag{8}$$

In addition we employ a mapping over the vertical coordinate η in the form:

$$\eta = 0.5\left(1 + \frac{\tanh\tilde{\eta}}{\tanh 1.5}\right) \tag{9}$$

where $-1.5 < \tilde{\eta} < 1.5$. Mapping (9) introduces a non-uniform spacing of the computational nodes in the vertical direction, with stretching in the middle of the domain (for $\tilde{\eta} \approx 0$ and $z \approx \eta \approx 0.5$) and clustering near boundaries (for $\tilde{\eta} \approx \pm 1.5$ and $z \approx \eta \approx 0$ and 1).

Equations (1)-(3) are discretized in a rectangular domain with sizes $0 < \xi < 6$, $0 < y < 4$, and $-1.5 < \tilde{\eta} < 1.5$ by employing a finite difference method of the second-order accuracy on a uniform staggered grid consisting of $360 \times 240 \times 180$ nodes. The integration is advanced in time by the second-order accuracy Adams-Bashforth method. Equation for the pressure is solved by an iteration procedure employing FFT over ξ, y coordinates and Gauss elimination method over the η-coordinate. At the lower plane boundary ($\eta = 0$) the no-slip (Dirichlet) condition for the velocity is prescribed. Thus, here the flow velocity coincides with the orbital velocities of particles in the surface water wave.At the upper boundary at $\eta = 1$ a no-slip condition for the velocity is prescribed with respect to the plane moving with non-dimensional velocity $1 - c$.The temperature deviation is set equal to zero both at the lower and upper boundaries. Periodical boundary conditions are prescribed at the side boundaries of the computational domain, at $x = 0$, 6 and $y = 0$, 4.

The flow velocity field is initialized as a weakly perturbed laminar Couette flow, $U_i = z\delta_{ix} + u_{if}$ ($i = x, y, z$) where u_{if} is a divergence-free isotropic, homogeneous random field with a broad power spectrum and amplitude of about 0.05. The initial temperature deviation field is put to zero.

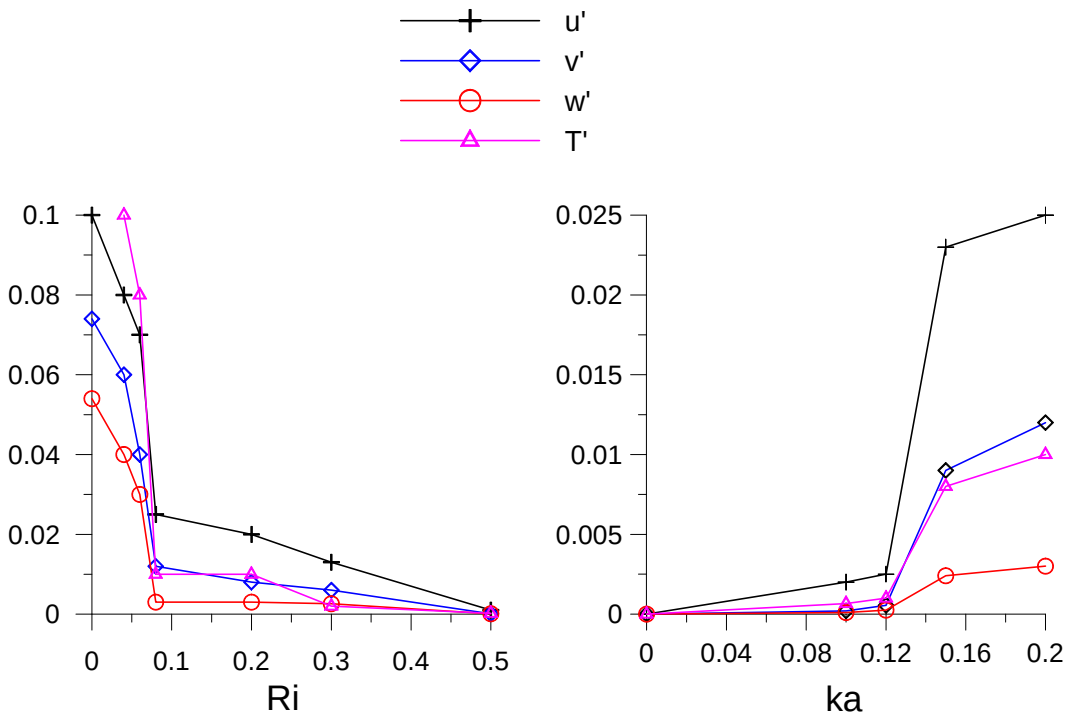

Fig. 3.

The integration is advanced in time until a statistically stationary flow regime sets in. Then sampling of the velocity and temperature fields is preformed at discrete time moments t_k, $k = 1,...,1000$ with increment $t_{k+1} - t_k = 0.2$. The averaging is performed over the spanwise y-coordinate, time, and the wave spatial period $\lambda = 1$ in the streamwise x-direction. The averaging over the wave length is performed as a window averaging.

Numerical results. DNS results show that the BL flow regime depends drastically on the choice of Richardson number, Ri, and wave slope, ka. We find that, for a given Reynolds number, there is a critical Richardson number $\mathrm{Ri_c}$, such that for $\mathrm{Ri} < \mathrm{Ri_c}$ there exists a stationary turbulent flow regime whereas for $\mathrm{Ri} > \mathrm{Ri_c}$ the flow turbulence is suppressed in the bulk of the domain due to the stabilizing effects of stratification and dissipation.

Figure 2 shows temporal development of the amplitudes of the fluctuations of velocity and temperature obtained in DNS for wave phase velocity c = 0.05 ($c/u_* \approx 2$) under the statistically stationary regime (for Ri = 0.04, ka = 0.2), decaying turbulence (for Ri = 0.08, ka = 0.1), and turbulence supported by the surface wave (for Ri = 0.08 and ka = 0.15 and ka = 0.2).

Figure 3 (left panel) shows that the fluctuation amplitudes decrease drastically as the Richardson number is increased and exceeds $\mathrm{Ri_c} \approx 0.08$ in DNS with wave slope ka = 0.2 and Re = 15000. The right panel of Fig. 2 (obtained for Ri = 0.08 and the same Re) shows also that there is a critical value of the wave slope, $ka_c \approx 0.12$, such that for $ka < ka_c$ the fluctuation amplitudes decay to zero whereas for $ka > ka_c$ they remain finite. DNS results (to be discussed below) show that in the case $\mathrm{Ri} > \mathrm{Ri_c}$ the fluctuations are most pronounced in the vicinity of the critical level, where the wave phase velocity coincides with the mean wind velocity. Therefore, in this case, the BL turbulence is pumped by the surface wave.

Figures 4 and 5 present contours of the instantaneous vorticity modulus field $\omega(x,y,z)$ in the central (x,z) and (y,z) planes (top and middle frames, respectively) and in (x,y) plane at z = 0.042 (bottom frame) obtained for Ri = 0.04 and Ri = 0.08 in DNS with wave slope ka = 0.2 and phase velocity c = 0.05. Figure 4 shows that in the case Ri = 0.04 the flow field is turbulent and characterized by numerous separation points at the wavy boundary. On the other hand, in the case Ri = 0.08 (Fig. 5) turbulent fluctuations are suppressed by stratification and the flow is quasi-laminar sufficiently far from the wavy boundary. However, the fluctuations are non-zero and the vorticity field in the vicinity of the wavy boundary is characterized by a complicated 3D-structure.

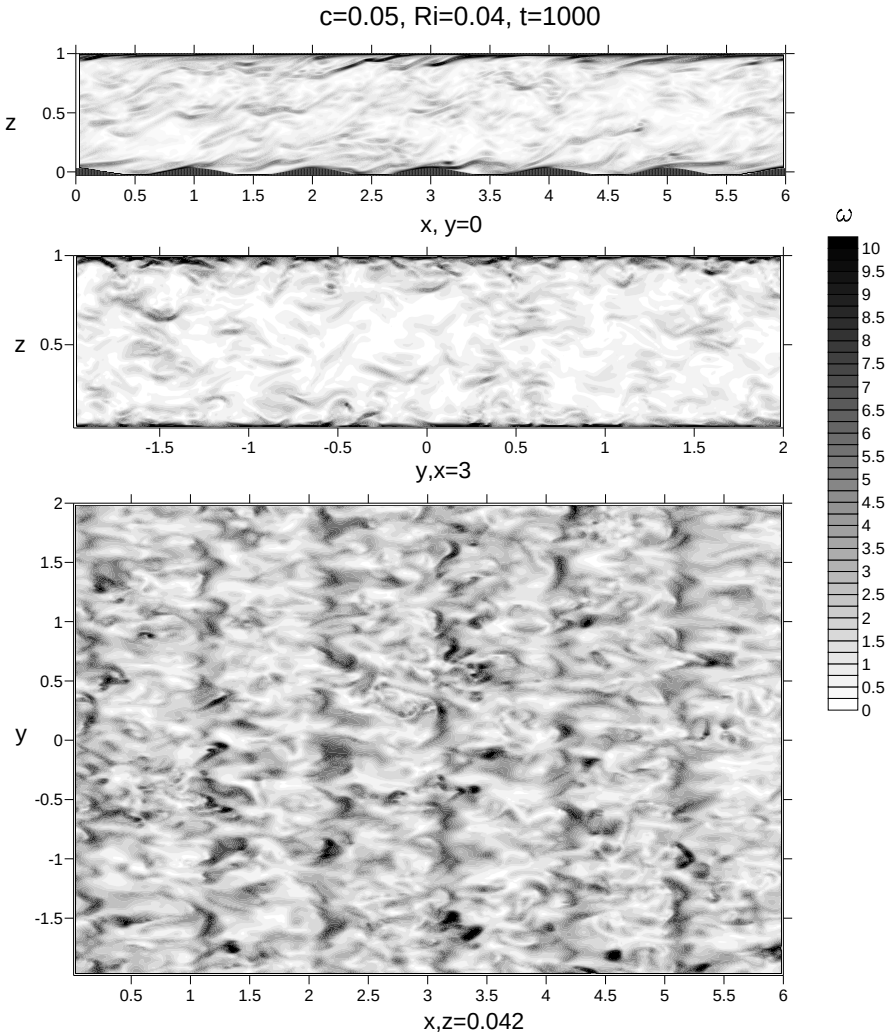

Fig. 4.

Figure 6 shows different properties of the stationary flow regime obtained in DNS for bulk Richardson number Ri = 0.04 and wave slope ka = 0.2, under the statistically stationary, turbulent flow regime. Figures 5a presents vertical profiles of the mean velocity and temperature fields, $< U_x >(z)$ and $< T >(z)$, and the gradient Richardson number,

$$Ri_g = Ri\frac{d < T > / dz}{(d < U_x > / dz)^2} = \frac{N^2}{(d < U_x > / dz)^2} \tag{10}$$

where $N(z)$ is the dimensionless buoyancy frequency. The figure shows that the mean velocity and temperature profiles have a similar, log-linear shape whereas the gradient Richardson number is about 0.1 for 0.1< z < 0.9 and decreases towards the walls. Figure 5b presents vertical profiles of the velocity and temperature fluctuations $u'_x(z)$, $u'_y(z)$, $u'_z(z)$, and $T'(z)$. Figures 5c and 5d show viscous stresses (11), and wave-induced (12) and turbulent momentum and heat fluxes (13):

$$P_{visc} = \frac{1}{\mathrm{Re}}\frac{d\left[< U_x >\right]}{d\eta}, \quad P^T_{visc} = \frac{1}{\mathrm{Re}\,\mathrm{Pr}}\frac{d < T >}{dz} \tag{11}$$

$$P_{turb} = -\left[< U'_x U'_z >\right] \qquad P^T_{turb} = - < T'U'_z > \tag{12}$$

$$P_{wave} = \left[\frac{\partial z}{\partial \xi} < U_x^2 + P >\right] - \left[\frac{\partial z}{\partial \eta} < U_x U_z >\right], \quad P^T_{wave} = \left[\frac{\partial z}{\partial \xi} < TU_x >\right] - \left[\frac{\partial z}{\partial \eta} < TU_z >\right] \tag{13}$$

Angle and square brackets in (11)-(13) denote averaging over y and t and over ξ – coordinate, respectively. Figures 5c and 5d show that the total momentum and heat fluxes,

$$P_{visc} + P_{wave} + P_{turb} = u_*^2, \qquad P^T_{visc} + P^T_{wave} + P^T_{turb} = T_* u_* \tag{14}$$

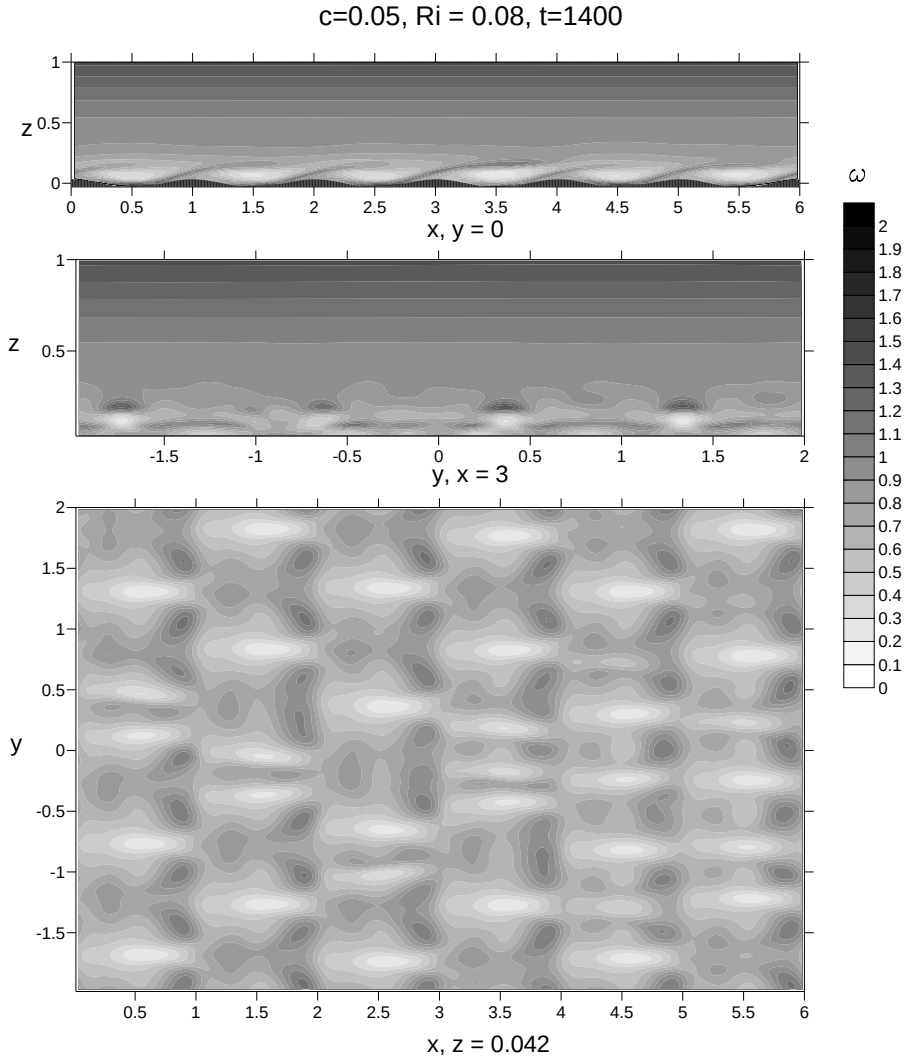

Fig. 5.

are practically independent on z. This shows that the momentum and heat fluxes are conserved in DNS.

Figures 7 presents vertical profiles of the mean velocity and temperature fields, $< U_x >(z)$ and $< T >(z)$, and the gradient Richardson number, $\mathrm{Ri_g}(z)$, evaluated from (10), (left) and the velocity and temperature fluctuations profiles (right) obtained in DNS for Ri = 0.08 for two different wave phase velocities c = 0.05 (top) and c = 0.2 (bottom) with *ka* = 0.2 under the regime where turbulence is supported by the surface wave. The figure shows that maxima of the fluctuation amplitudes are located in the vicinity of the critical layer, at such z_c-level where $< U_x >(z_c) = c$, which is shifted away from the wavy surface for larger *c*.

Figure 8 shows the profiles of turbulent momentum and heat fluxes, $< U_x' U_z' >(z)$ and $< T' U_z' >(z)$, obtained in DNS for different Richardson numbers and wave slopes. The figure shows that the fluxes are reduced for larger Ri and smaller *ka*. Under the statistically stationary turbulent regime, for $\mathrm{Ri} < \mathrm{Ri_c}$, the fluxes saturate and do not depend on *z* in the logarithmic BL region. For sufficiently large Richardson number, when $\mathrm{Ri} > \mathrm{Ri_c}$ the fluxes remain non-zero in the vicinity of the critical layer, where the mean velocity coincides with the wave phase velocity.

Conclusion. We performed DNS of turbulent, stably-stratified boundary layer (BL) flow over a wavy water surface and considered the effect of stratification on the properties of the flow for different wave slope and celerity. Our results show that if the Richardson number is sufficiently small, there exists a statistically stationary, turbulent BL flow regime. if the Richardson number is sufficiently large the wind flow turbulence is suppressed under the stabilizing effect of stratification, and velocity fluctuations in the BL decay to zero, in the case of a sufficiently small

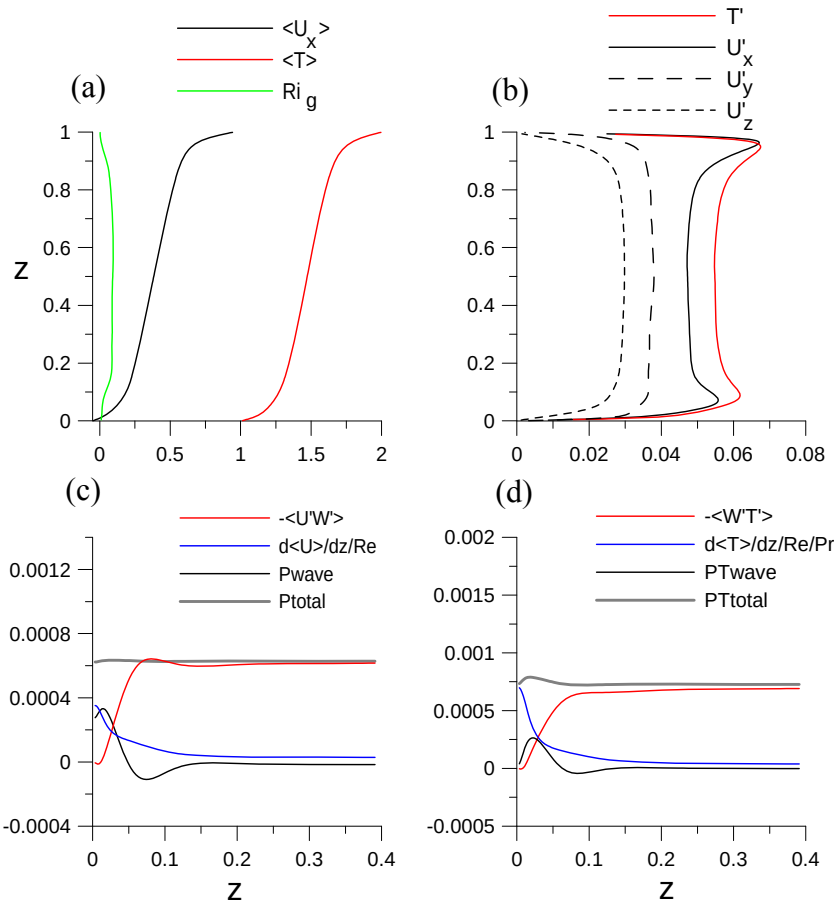
(a)
<U_x>
<T>
Ri g
Z
(b)
T'
U'x
U'y
U'z
(c)
-<U'W'>
d<U>/dz/Re
Pwave
Ptotal
Z
(d)
-<W'T'>
d<T>/dz/Re/Pr
PTwave
PTtotal
Z

Fig. 6

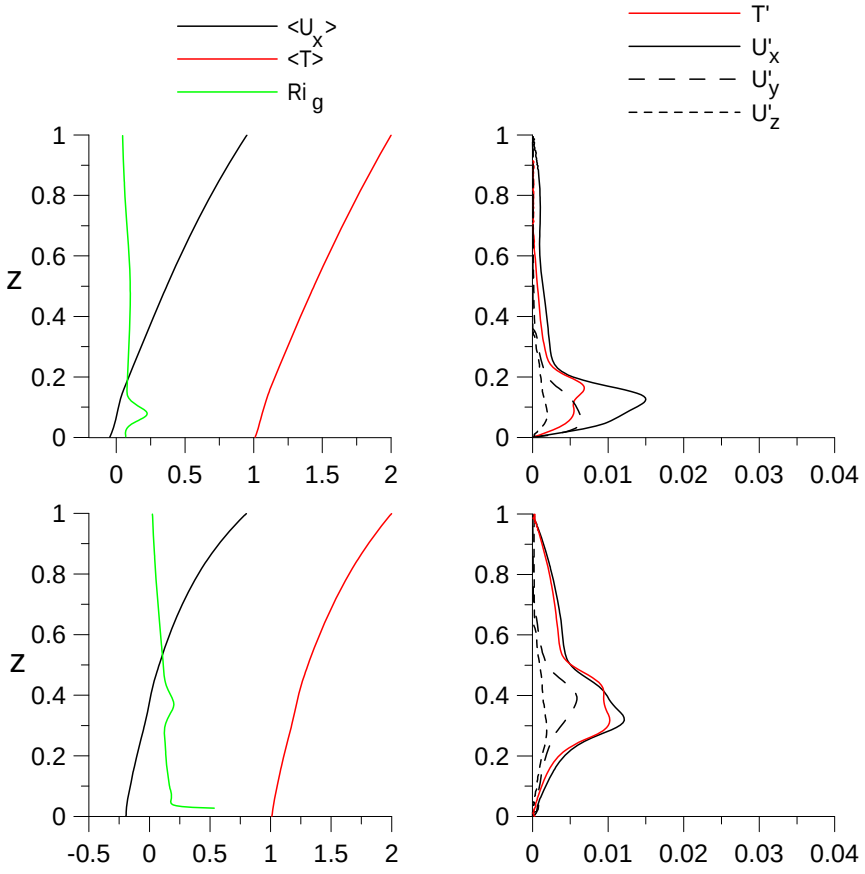
<U_x>
<T>
Ri g
T'
U'x
U'y
U'z
Z
Z

Fig. 7.

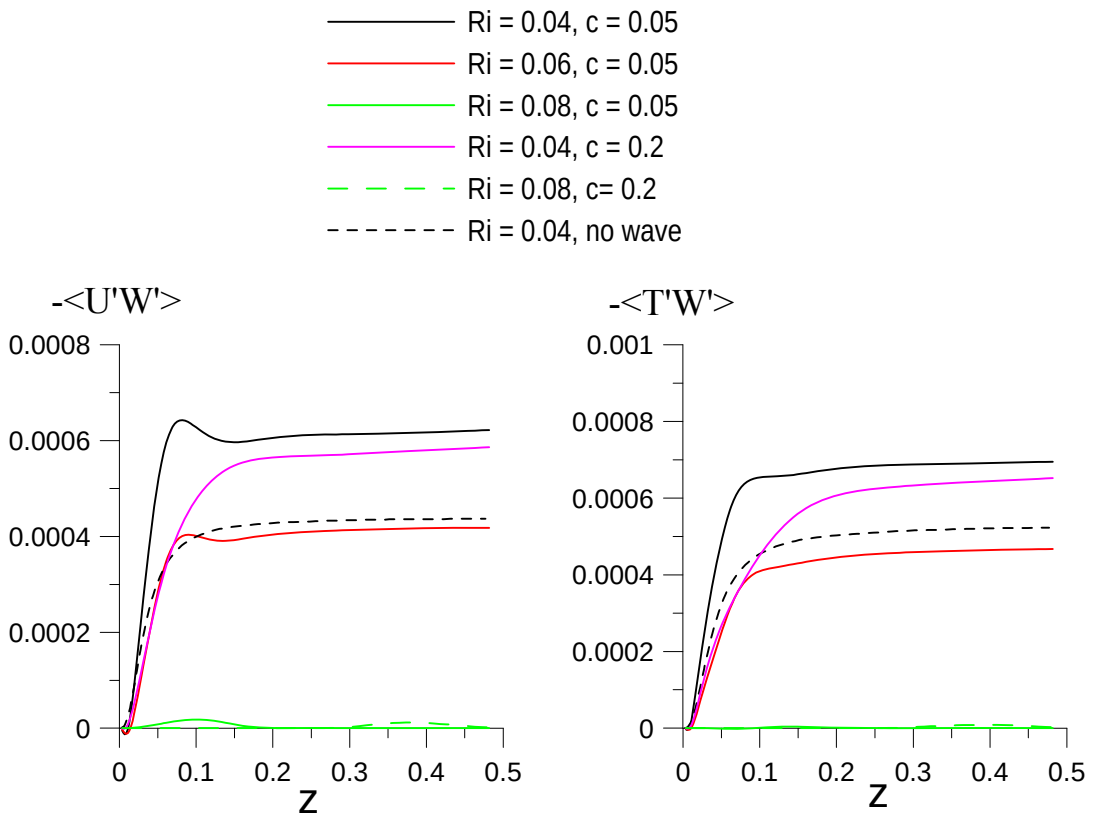

Fig. 8.

wave slope. However, the velocity fluctuations remain finite (non-zero) if the wave slope is sufficiently large. Hence, the turbulence is supported by the surface wave in this case. The mechanism of this "pumping" of turbulence by the surface wave needs further investigation. One possible scenario is that the 2D Tolmienn-Shlichting (TS) wave is first excited by direct forcing due to the surface wave, and futher a spanwise instability of TS wave develops which creates a 3D structure of the velocity field in the vicinity of the critical layer.

Acknowledgement. This work was supported by the Government of the Russian Federation (contract No. 11.G34.31.0048) and by RFBR (project Nos. 13-05-91175, 14-05-00367).

References

1. Fairall C.W., Bradley E.F., Hare J.E., Grachev A.A., Edson J.B. Bulk parameterization of air–sea fluxes: updates and verification for the COARE algorithm // Journal of Climate, 2003. V. 16. № 74. P. 571–591.
2. Reul N., Branger H., Giovanangeli J.-P. Air flow separation over unsteady breaking waves // Phys. Fluids, 1999. V. 11. P. 1959–1961.
3. Monin, A. S. and Yaglom, A. M.: Statistical fluid dynamics. V.1, Gidrometeoizdat, St. Petersburg, 1992.
4. Druzhinin O.A., Troitskaya Yu. I., Zilitinkevich S.S. Direct numerical simulation of a turbulent wind over a wavy water surface // J. Geophys. Res. 2012. V. 117. C00J05. doi:10.1029/2011JC007789. 16PP.
5. Phillips, O.M.: *The dynamics of the upper ocean*, 2nd ed., Cambridge 1977.